

# Integration of Probabilistic Atlas and Graph Cuts for Automated Segmentation of Multiple Sclerosis lesions

Francesca Galassi, Olivier Commowick, Christian Barillot

► **To cite this version:**

Francesca Galassi, Olivier Commowick, Christian Barillot. Integration of Probabilistic Atlas and Graph Cuts for Automated Segmentation of Multiple Sclerosis lesions. ISMRM 2018 - International Society for Magnetic Resonance in Medicine, Jun 2018, Paris, France. pp.1-6. <hal-01823801>

**HAL Id: hal-01823801**

**<https://hal.archives-ouvertes.fr/hal-01823801>**

Submitted on 27 Jun 2018

**HAL** is a multi-disciplinary open access archive for the deposit and dissemination of scientific research documents, whether they are published or not. The documents may come from teaching and research institutions in France or abroad, or from public or private research centers.

L'archive ouverte pluridisciplinaire **HAL**, est destinée au dépôt et à la diffusion de documents scientifiques de niveau recherche, publiés ou non, émanant des établissements d'enseignement et de recherche français ou étrangers, des laboratoires publics ou privés.

## TITLE

Integration of Probabilistic Atlas and Graph Cuts for Automated Segmentation of Multiple Sclerosis lesions

## AUTHORS

Francesca Galassi<sup>1</sup>, Olivier Commowick<sup>1</sup>, and Christian Barillot<sup>1</sup>

<sup>1</sup>INRIA, CNRS, IRISA UMR 6074, VISAGES ERL U-1228, F-35000, Rennes, France

## INTRODUCTION

We propose a framework for automated segmentation of Multiple Sclerosis (MS) lesions from MR brain images. It integrates *a priori* tissues and MS lesions information into a Graph-Cuts algorithm for improved segmentation results.

## METHOD

*Pre-processing.* The method requires three MR sequences per subject: T1-w, T2-w and FLAIR. MR images are first denoised<sup>1</sup>, rigidly registered towards the T1-w image<sup>2</sup>, skull-stripped<sup>3</sup> and bias corrected<sup>4</sup>. Then, their intensities are normalized by applying the decile normalization method proposed by Nyul et al.<sup>5,6</sup>.

A probabilistic atlas (i.e. CSF, WM, GM and MS lesion probability maps intensity normalized for the four classes, Figure 1) is registered into the subject space. The T1-w template image is registered to the T1-w subject image using a linear registration, based on a block-matching algorithm<sup>2</sup>, followed by a dense non-linear registration<sup>7</sup>.

*Segmentation method.* We adopt a Graph-Cuts segmentation approach, where the two terminal nodes, *source* and *sink*, respectively represent the MS lesions, or *object* class, and the Normal Appearing Brain Tissues (NABT), or *background* class<sup>8</sup>. Given the set of nodes  $I$  and the set of connections  $N$  between two nodes  $\{i, j\}$ , the GC algorithm minimizes an energy function  $E(V)$ , where  $V$  is the *object* segmentation:

$$E(V) = \sum_{\{i,j\} \in N} B_{\{i,j\}} + \alpha \sum_{i \in I} R_i(V_i).$$

The boundary term  $B_{\{i,j\}}$  reflects the similarity of neighbouring voxels  $\{i,j\}$ , and the regional term  $R_i(\cdot)$  refers to the probability for  $i$  to fit into the *object* and *background* models. We

compute the boundary weights using the spectral gradient<sup>8</sup> and the *object* and *background* weights as described below.

We model the NABT with a 3-class Gaussian Mixture Model. We estimate the NABT GMM using tissue probability maps with a robust EM<sup>9</sup>, which optimizes a trimmed likelihood to be robust to the presence of outliers (i.e. lesions). Then, we evaluate the Mahalanobis distance  $Z^2$  between each voxel  $i$  and each tissue class  $m$ . Assuming that  $Z^2$  follows a  $\chi^2_m$  distribution, the *p-value* for a voxel  $i$  is obtained as

$$p_{im} = 1 - F_{\chi^2_m}(Z^2)$$

$p_{im}$  represents the probability that the voxel  $i$  does not fit into a class  $m$  of the NABT GMM.

Voxels that fit into the NABT GMM must have a high *background* weight  $W_{iB}$ . We formulate the equation for computing  $W_{iB}$  to include both  $p_{im}$  and *a priori* MS lesion information  $P_{iMS}$  as

$$W_{iB} = \beta(1.0 - \min(p_{im})) + (1 - \beta)(1.0 - P_{iMS}),$$

where the parameter  $\beta$  controls the amount of information from the Mahalanobis distance and the prior.  $\min(p_{im})$  is the lowest *p-value* among the  $m$  classes for a voxel  $i$ . The parameter  $\beta$  was set to 70%.

We formulate the *object* weights to include information from the MS lesion prior, the Mahalanobis distance and the hyper-intensities on T2-w and FLAIR images:

$$W_{oi} = \min(P_{iO}, W_{T2}, W_{flair}),$$

where

$$P_{iO} = \beta \min(p_{im}) + (1 - \beta) P_{iMS}$$

$W_{T2}, W_{flair}$  are fuzzy weights derived from the T2-w and FLAIR hyper-intensities<sup>8</sup>.

*Post-processing.* A candidate lesion is discarded if one of the following conditions is verified: *i*) it is not sufficiently located within the WM, *ii*) it touches the brain mask border, *iii*) its size is lower than 3mm<sup>3</sup>.

## RESULTS

We evaluated the method on 37 MS subjects. Each subject included T1-w, T2-w and FLAIR images. The ground truth was computed using the LOP STAPLE method<sup>12</sup> on six independent manual segmentations per patient. Results are illustrated in Figure 2. The average Dice Similarity Coefficient (DSC) was 0.578, the average Positive Predictive Value (PPV) was 0.711. An example of segmentation result (*without* and *with* priors) is illustrated in Figure 3.

The computation time to process a subject on a laptop with an Intel Core i7 CPU 2.40GHz (8 cores) was approximately 10 minutes.

## DISCUSSION

Results indicate good performance of the proposed method. Three of the MS subjects with low lesion load and low number of lesions obtained a DSC lower than 0.3. This can be partially explained by the low experts' agreement, which becomes more relevant for a small lesion load. When compared to a Graph-Cuts approach that does not include knowledge from MS lesion priors, our approach shows generally improved performance (average DSC=0.480 on the same dataset).

## CONCLUSION

We propose a framework that incorporates tissues and MS lesions probability maps into a Graph-Cuts approach for MS lesions segmentation. Results indicate that integrating *a priori* information with the information derived from the images can improve the segmentation outcome. The performance of the proposed method relies on the accuracy of the probabilistic atlas and parameters that must be accurately tuned on a training dataset. The method can be easily adapted to be used with different MR sequences (e.g. PD images).

## REFERENCES

1. Coupe, P. *et al.* An optimized blockwise nonlocal means denoising filter for 3-D magnetic resonance images. *IEEE Trans. Med. Imaging* **27**, 425–441 (2008).
2. Commowick, O., Wiest-Daesslé, N. & Prima, S. Block-matching strategies for rigid registration of multimodal medical images. in *2012 9th IEEE International Symposium on Biomedical Imaging (ISBI)* 700–703 (2012).  
doi:10.1109/ISBI.2012.6235644
3. Manjón, J. V. & Coupé, P. volBrain: An Online MRI Brain Volumetry System. *Front. Neuroinformatics* **10**, (2016).
4. Tustison, N. J. *et al.* N4ITK: improved N3 bias correction. *IEEE Trans. Med. Imaging* **29**, 1310–1320 (2010).
5. Nyul, L. G., Udupa, J. K. & Zhang, X. New variants of a method of MRI scale standardization. *IEEE Trans. Med. Imaging* **19**, 143–150 (2000).
6. Shah, M. *et al.* Evaluating intensity normalization on MRIs of human brain with multiple sclerosis. *Med. Image Anal.* **15**, 267–282 (2011).
7. Commowick, O., Wiest-Daesslé, N. & Prima, S. Automated diffeomorphic registration of anatomical structures with rigid parts: application to dynamic cervical MRI. *Med. Image Comput. Comput.-Assist. Interv. MICCAI Int. Conf. Med. Image Comput. Comput.-Assist. Interv.* **15**, 163–170 (2012).
8. García-Lorenzo, D., Lecoœur, J., Arnold, D. L., Collins, D. L. & Barillot, C. Multiple sclerosis lesion segmentation using an automatic multimodal graph cuts. *Med. Image Comput. Comput.-Assist. Interv. MICCAI Int. Conf. Med. Image Comput. Comput.-Assist. Interv.* **12**, 584–591 (2009).
9. García-Lorenzo, D., Prima, S., Arnold, D. L., Collins, D. L. & Barillot, C. Trimmed-likelihood estimation for focal lesions and tissue segmentation in multisequence MRI for multiple sclerosis. *IEEE Trans. Med. Imaging* **30**, 1455–1467 (2011).
10. Commowick, O., Cervenansky, F. & Ameli, R. *MSSEG Challenge Proceedings: Multiple Sclerosis Lesions Segmentation Challenge Using a Data Management and Processing Infrastructure.* (2016).
11. Guimond, A., Meunier, J. & Thirion, J.-P. Average Brain Models. *Comput Vis Image Underst* **77**, 192–210 (2000).
12. A Logarithmic Opinion Pool Based STAPLE Algorithm for the Fusion of Segmentations With Associated Reliability Weights - IEEE Journals & Magazine. Available at: <http://ieeexplore.ieee.org/document/6832625/>. (Accessed: 5th November 2017)

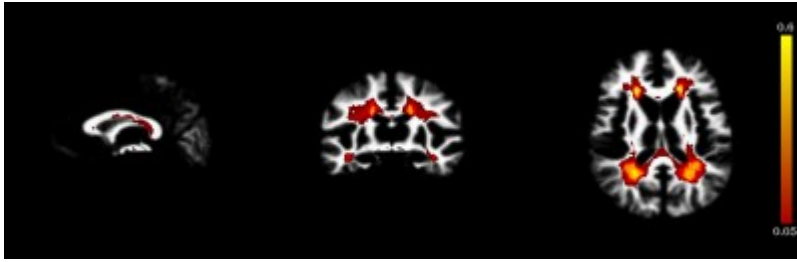


Figure 1. MS lesion probability map overlaid the WM probability map. MS lesion priors were generated from 89 subjects with manually annotated lesions, with lesion loads from  $0.1\text{cm}^3$  to  $64\text{cm}^3$  and a total number of lesions equal to 7927. The dataset included the 15 MS subjects from the MICCAI'16 training database<sup>10</sup> and 74 MS subjects from an MS-SPI database. Tissue priors were generated using the method proposed by Guimond et al.<sup>11</sup>, which construct models representing the average intensity and shape of the images. Registration involved a linear registration, based on a block-matching algorithm<sup>2</sup>, followed by a dense non-linear registration<sup>7</sup>.

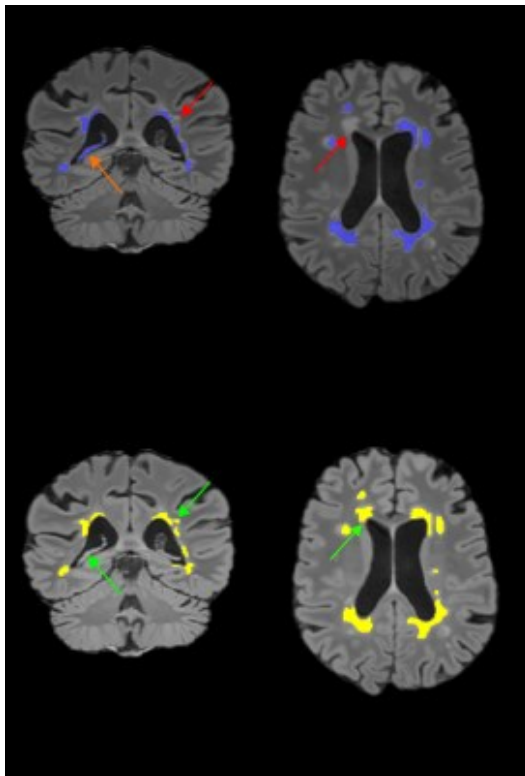


Figure 2. MS lesions as segmented using the proposed method, without (top) and with (bottom) MS lesion priors in the computations of the term weights. Results are overlaid the FLAIR image. With the use of the MS lesion priors missing lesions (red arrows) can be detected (green arrows) and false positive (orange arrows) can be removed.

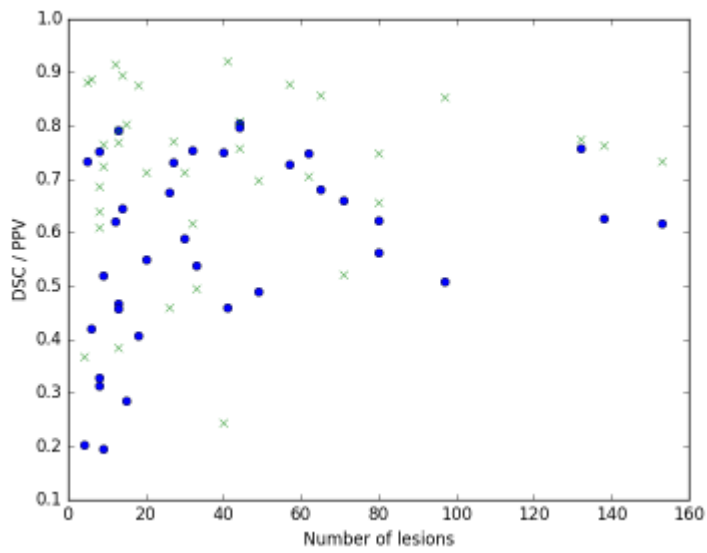
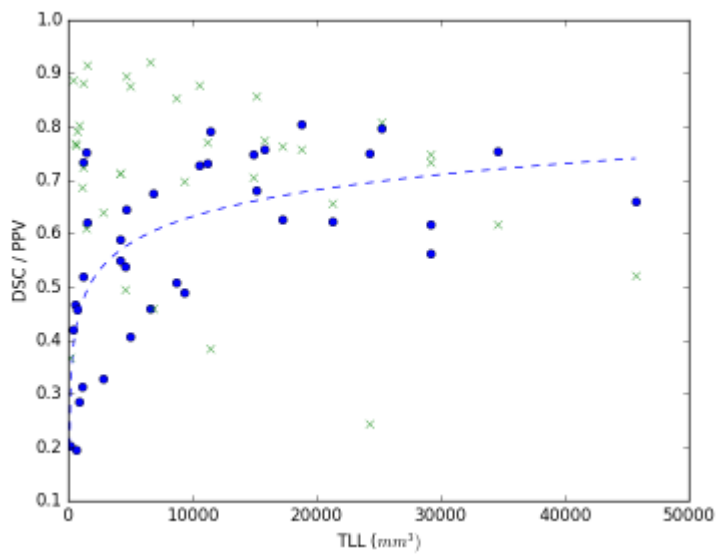


Figure 3. a) DSC (blue markers), PPV (green markers) and Total lesion load (TLL) per patient. Lesion loads varied from  $0.1\text{cm}^3$  to  $46\text{cm}^3$ . b) DSC (blue markers), PPV (green markers) and number of lesions per patient.